CHAPTER 14

COMPUTATIONAL STUDY OF UV-INDUCED EXCITATIONS OF DNA FRAGMENTS

MANOJ K. SHUKLA AND JERZY LESZCZYNSKI*

Computational Center for Molecular Structure and Interactions, Department of Chemistry, Jackson State University, Jackson, MS 39217, USA

Abstract: The recent experimental and theoretical results in elucidating the structures and properties of ultraviolet (UV)-induced electronic excitations of DNA fragments and related analogs are discussed. Although, the electronic absorption maxima of nucleic acid bases are in the UV region of the energy spectrum, these genetic molecules are highly photostable. The observed photostability is the outcome of the extremely short excited state life-times. This fundamental characteristic of nucleic acid bases on the other hand is attained by the ultrafast nonradiative decay through internal conversion. Recent theoretical investigations unambiguously show that excited state geometries are generally nonplanar, though the amount of nonplanarity depends on the level of theory used in the calculation. It is also evident that conical intersections involving ground and excited state potential energy surfaces are instrumental for such nonradiative deactivation. Though, theory and experiments are complementary to each other, but the experimental progress in studying excited state properties are far ahead compared to the theoretical methods. For example, it is still very challenging for an extensive investigation of excited state properties of systems like nucleic acid bases at multi-configurational theoretical levels and with large basis sets augmented with diffuse functions. The theoretical and computational bottleneck impedes the investigation of effect of stacking interaction, which is of the fundamental importance for DNA, at the reliable theoretical level. However, we hope that with the theoretical and computational advances such investigations will be possible in near future

Keywords: DNA Fragments, Base Pair, Nonradiative Decay, Excited State, Ab Initio

14.1. INTRODUCTION

The deoxyribonucleic acid (DNA) has three important components: (1) purine and pyrimidine bases, (2) deoxyribose sugar and (3) phosphate group. The adenine and guanine belong to the purine class of nucleic acid bases while thymine and cytosine

* Corresponding author, e-mail: jerzy@ccmsi.us

M. K. Shukla, J. Leszczynski (eds.), Radiation Induced Molecular Phenomena in Nucleic Acids, 369–393.

belong to the pyrimidine class of bases. In ribonucleic acid (RNA) thymine is replaced with uracil (see Figure 14-1 for structure and atomic numbering schemes of DNA and RNA bases). DNA is known as genetic carrier where information is stored in the form of specific patterns of sequence of hydrogen bonds formed between purine and pyrimidine bases (adenine with thymine and guanine with cytosine). It was Avery et al. [1] who in 1944 discovered that DNA was the genetic agent responsible for the heredity and this theory was confirmed only in 1952 by Hershey and Chase [2]. The helical nature of fibrous DNA was demonstrated using X-ray diffraction study [3, 4] and double helical structure was discovered by Watson and Crick [5]. These discoveries opened new era of biological research called molecular biology. A great deal of basic information about structures of nucleic acids can be found in a recent review article by Schneider and Berman [6] published in the second

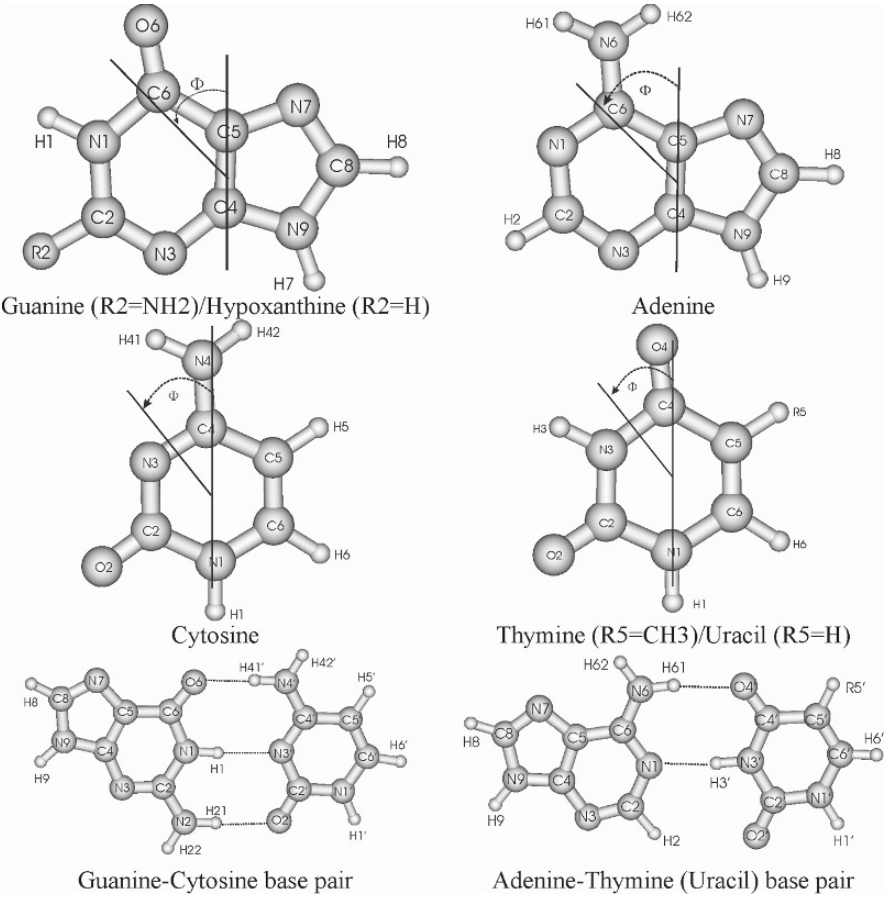

Figure 14-1. Structure and atomic numbering schemes of nucleic acid bases and Watson-Crick base pairs. The Φ represents the transition moment direction according to the DeVoe-Tinoco convention [11]

volume of the current book series "Challenges and Advances in Computational Chemistry and Physics".

Remarkable photophysical properties have been endowed to DNA to combat the photodamage. It is well known that nucleic acid bases (NABs) absorb ultraviolet (UV) radiation efficiently. But quantum efficiency of the radiative emission is extremely poor in aqueous solution at room temperature and most of the absorbed energy is released in the form of ultra-fast nonradiative decay in the subpicosecond time scale and the inclusion of the bulky group on NABs increases the time scale [7]. It is expected that life on earth started in an extremely harsh environment, where there were abundant of UV-irradiation. Since absorption profile of NABs lies in the UV-spectral range and the fact that electronic excited states are very favorable for photoreactions; the stability requirement necessiated genetic materials with very short electronic excited state life-time. However, UV and ionizing radiation are dangereous. Alteration in DNA structure may lead to mutation by producing a permanent change in the genetic code. The exact cause for mutation is not known, but several factors e.g. environment, irradiation etc., may contribute towards it. The formation of pyrimidine dimers between adjacent thymine bases on the same strand results in the most common UV-induced DNA damage. Kohler and coworkers [8], based on the femtosecond time-resolved IR spectroscopic study on thymine oligodeoxynucleotide $(dT)_{18}$ and thymidine 5′-monophosphate (TMP), have recently shown that thymine dimerization is an ultrafast process usually occurs in the femtosecond time scale, where the formation of photodimer from the initially excited singlet $\pi\pi^*$ state of thymine is barrierless. However, the proper geometrical orientation of stacked thymine pairs is the necessary requirement for the formation of photodimer. Recent investigations suggest that low energy radiation (even less than 3 eV) may also cause strand breaks in the nucleic acid polymers [9, 10]. Interesting results devoted to the experimental and theoretical discussion of low energy electron induced DNA damage are presented in the current volume (see Chapters 18–21).

Spectroscopic methods have long been used to study structures and properties of nucleic acids. Although, the fluorescence of NABs at in aqueous solution is very poor (fluorescence quantum yield being around 10^{-4} or less) [7, 11], on the other hand, the fluorescence were obtained from the protonated forms of bases in the room temperature solution [12–14]. The first low temperature work on nucleic acids was reported in 1960 [15], while the phosphorescence of nucleic acids was reported for adenine derivatives in 1957 [16]. The first results on isolated monomers were obtained in 1962 by Longworth [17] and in 1964 by Bersohn and Isenberg [18]. Initially low temperature measurements were performed using a frozen aqueous solution, but due to the inherent problems in such matrices, most investigations were turned to polar glasses such as ethylene or propylene glycols usually mixed with equal volumes of water [19]. A great deal of discussion on the photophysical properties of DNA fragments based on the earlier experimental work can be found in the excellant review article by Eisinger and Lamola published in 1971 [19] and that by Callis in 1983 [11]. The latter work also summarizes theoretical transition energy

data based on the semiempirical results. Recently, state-of-the-art spectroscopic investigations have been performed to study ground and excited state structures and dynamics of NABs mostly in the supersonic jet-cooled beam and in some cases in an aqueous solution at the room temperature [7, 20, 21]. The nonradiative decay mechanisms have also been investigated using the high levels of theoretical calculations [22–36]. Discussion about the different investigations can be found in the recent review articles [7, 20, 21, 37]. It is becoming evident that the excited state structural nonplanarity promotes conical intersection between the ground and excited states and therefore provides suitable trail for the ultrafast nonradiative decays in genetic molecules. Great deal of attention has been paid in the current book where several chapters are devoted in unravelling the underlying mechanism for the ultrafast nonradiative decay in NABs.

14.2. GROUND STATE STRUCTURES AND PROPERTIES OF NUCLEIC ACID BASES AND BASE PAIRS

Depending upon the environment, nucleic acid bases can have different tautomeric forms. The prototropic tautomerism involving the N9 and N7 sites of purines (adenine and guanine) and the N1 and N3 sites of pyrimidine (cytosine) are blocked in nucleosides and nucleotides due to the presence of sugar at the N9 and N1 sites of purines and pyrimidines, respectively. However, the possibility of the formation of other tautomeric forms (enol and imino) is not hindered in these species (nucleosides and nucleotides). Thorough discussion about different ground state properties including stacking interactions and interactions with metal cations and solvents can be found in some recent review articles [38, 39] and in the second volume of the current book series [40]. Therefore, only brief description of ground state properties of NABs and base pairs are presented here.

Recent high level experimental and theoreical results suggest the existence of very complex tautomeric behaviour in guanine. Using the resonance enhanced multi-photon ionization spectroscopic technique, the four tautomers of guanine namely keto-N9H, keto-N7H, enol-N9H, and enol-N7H have been suggested in the laser desorbed jet-cooled beam of guanine [41, 42]. However, for guanine trapped in helium droplets only keto-N9H, keto-N7H and cis- and trans forms of the enol-N9H tautomer of guanine have been revealed by Choi and Miller [43]. This conclusion was based on the agreement between the experimental infra-red (IR) spectral data of guanine trapped in helium droplets and that of the theoretically computed vibrational frequencies of guanine tautomers at the MP2 level using the 6-311++G(d,p) and aug-cc-pVDZ basis sets. The results of Choi and Miller prompted Mons et al. [44] to reassign their previous R2PI data and according to the new assignment, the enol-N9H-trans, enol-N7H and two rotamers of the keto-N7H-imino tautomers of guanine are present in the supersonic jet-beam. It should be noted that imino tautomers of guanine are about 8.0 kcal/mol less stable than the most stable keto-N7H tautomer in the gas phase at the MP2/6-311++G(d,p)//B3LYP/6-311++G(d,p) level [45]. Thorough discussion about guanine tautomerism and that of the R2PI spectra has

already been made by Prof. Mons in the previous chapter. Recent experimental investigation along with theoretical calculation suggest that adenine has three tautomers namely N9H, N7H and N3H in the dimethylsulfoxide solution; the N9H being the major form while N7H and N3H are the minor tautomeric forms [46]. It should be noted that in earlier experimental investigations only two tautomeric forms of adenine (N9H and N7H) have been suggested [47–49]. The N9H form was the major tautomer, while the relative population of the minor N7H form was found to be the environment dependent [47–49]. Recent theoretical investigations show that the N9H tautomer of adenine has the global minima, the stability of the N3H and N7H tautomers is almost similar [50, 51].

The purine metabolic intermediate hypoxanthine is structurally similar to guanine and can be formed by the deamination of the latter [52]. It is also found as a minor purine base in transfer RNA [53, 54]. During DNA replication hypoxanthine can code for guanine and can pair with cytosine [55]. Similar to guanine, hypoxanthine also shows keto-enol and prototropic (N9H-N7H) tautomerism [56, 57], but the concentration of enol tautomer in guanine is significantly larger than that in hypoxanthine [57]. The tautomeric equilibria in guanine are much more complex than that in the hypoxanthine. However, it should be noted that much attention has been paid to understand the physical and chemical properties of guanine than hypoxanthine. The dominance of the keto-N7H tautomer over the keto-N9H form (hydrogen being at the N1 site in both forms) of hypoxanthine has been suggested in the quantum chemical studies in the gas phase [58–61], matrix isolation studies [56, 57], photoelectron spectra [62] and NMR studies in the dimethylsulfoxide [47]. The existence of a small amount of the enol-N9H form of hypoxanthine has also been suggested in both theoretical and experimental investigations [56–61]. Theoretical calculations suggest that under aqueous solvation, the keto-N9H form is favored over the keto-N7H form and the enol-N9H form is largely destabilized [58–61]. The UV-spectroscopic study in water also predicts the domination of the keto-N9H form over the keto-N7H form [63]. In a crystalline environment, hypoxanthine exists as the keto-N9H tautomeric form [64]. Theoretically, the water assisted proton transfer barrier height corresponding to the keto-enol tautomerization of hypoxanthine was found to be reduced significantly compared to tautomerization without a water molecule [58, 59]. It was also shown that the transition state corresponding to a proton transfer from the keto form to the enol form of the hydrated species has a zwitterionic structure [58, 59]. These results were found to be in accordance with the molecular dynamics simulation study of proton transfer in a protonated water chain which was described in the form of the collective movement of protons in a water chain involving either the H_3O^+ or $H_5O_2^+$ [65].

Among pyrimidine bases, cytosine shows significant tautomeric acitivity. In argon and nitrogen matrices, it exists as a combination of amino-oxo (N1H) and amino-hydroxy forms; the tautomeric equilibrium being shifted towards the latter form [66, 67]. In microwave studies, the amino-oxo, imino-oxo, and amino-hydroxy forms of cytosine are revealed [68] and in the aqueous solution only amino-oxo forms (N1H and N3H) are present [69]. In a recent REMPI study of laser desorbed jet cooled

cytosine, Nir et al. [70] have shown the existence of keto and enol tautomers of cytosine. The matrix isolation study has also indicated the existence of imino-oxo tautomer in 1-methyl and 5-methylcytosine [71, 72]. In the crystalline environment the existence of only amino-oxo-N1H form is revealed [73]. Theoretically, upto the CCSD(T) level of theory has been used to determine the relative stability among different tautomers of cytosine [74, 75]. In the gas phase the amino-hydroxy tautomer is predicted to be the most stable; however, under aqueous solvation tautomeric stability is found to be shifted to the canonical amino-oxo form [75, 76]. Although, uracil and thymine exist mainly in the oxo-tautomeric form [37–39], the aqueous soltion of 5-chlorouracil at room temperature is suggested to possesses small amount of enol tautomeric form [77]. On the basis of the UV/Vis absorption and fluorescence data, Morsy et al. [78] have suggested the presence of small amount of the enol form of thymine, but Hobza group [79] does not support the utility of such measurement in tautomeric detection. It should be noted that the presence of small amounmt of minor tautomeric form of thymine in aqueous solution is not completely ruled out from theoretical calculations [79].

The six-membered ring of NABs is revealed theoretically to have significantly large conformational flexibility [80, 81]. The amino group of the NABs are nonplanar. Of the NABs, guanine exhibits the largest degree of pyramidalization [38, 39, 82]. The amino group pyramidalization originates from the partial sp^3 hybradized nature of the amino nitrogen. Using the vibrational transition moment direction analysis, Dong and Miller [83] have indicated experimentally the pyramidal nature of amino group in adenine and cytosine.

For a given system, the amount of energy released when an electron (proton) is added to the molecule is called electron (proton) affinity. The energy difference between the neutral and anionic (cationic) forms of the molecule yields the electron (proton) affinity. On the other hand, the amount of energy required to remove an electron from a molecule is called the ionization potential. The ionization potential is computed as the energy difference between the cationic and neutral forms of the molecule. Based on the experimental and theoretical data, the adiabatic valence electron affinity for pyrimidine bases has been estimated to be in the range of 0–0.2 eV while that for guanine and adenine it is about –0.75 and –0.35 eV, respectively [84]. Guanine has the lowest ionization potential among NABs and in general purines have lower and pyrimidines have higher ionization potentials [85–90]. Due to the low ionization energy, guanine is the most susceptible of the NABs to one electron oxidation under irradiation. The protonation and deprotonation properties of NABs have also been studied both theoretically [91–93] and experimentally [94–96]. Podolyan et al. [91] computed proton affinities of all nucleic acid bases up to the MP4(SDTQ) level and found that the computed proton affinities are very close to the experimental data; the computed error was found to be within the 2.1%.

At the HF and DFT level, the ground state geometries of the Watson-Crick (WC) base pairs are generally planar including the amino group [38, 39, 97–100]. However, at the MP2 level the amino groups of the WC GC and AT base pairs are revealed pyramidal with smaller basis set, but with larger basis sets the

corresponding group of the AT base pair was found almost planar [99, 101]. It has been suggested that the nonplanarity of the GC base pair may enhance the stacking of bases on the strand and may increase the stability of the helix [101]. The structural properties of different reverse Watson-Crick (RWC), Hoogsteen (H) and reverse Hoogsteen (RH) base pairs have also been investigated theoretically, and the geometries of some of them have been found to be nonplanar [38, 39, 102]. Recently, the energetics of hydrogen bonded and stacked base pairs were studied up to the CCSD(T) level [103–107]. Kumar et al. [108, 109] have recently investigated the adiabatic electron affinities of GC, AT and hypoxanthine-cytosine base pairs at the DFT level and found the significant increase in the electron affinity of the AT base pair under polyhydrated environments. A comprehensive investigation of structure and properties of deprotonated GC base pair was recently performed by Schaefer and coworkers [110].

14.3. EXCITED STATE PROPERTIES

14.3.1. Electronic Transitions of DNA Bases

It is generally known that the 260 and 200 nm absorption bands of purines consist of two transitions with nonparallel transition dipole moments and the relative intensity and positions of these peaks are dependent on the environment [11, 111, 112]. Occasionally, a weak transition near 225 nm is also observed which is considered to be the weak $\pi\pi^*$ or the $n\pi^*$ transition [11, 113]. Five electronic transitions in the UV region are generally obtained for guanine in different environments [11, 114]. The first transition lies near 4.51 eV (275 nm) and second is located near 4.96 eV (250 nm) region; the intensity of the latter is stronger than the former one [115–117]. The third transition near 5.51 eV (225 nm) is very weak and is rarely observed. This transition has been only observed in the protonated form of guanine and in the electronic spectra of crystalline guanine and 9-ethylguanine [115]. Although, it has also been observed in the CD spectra, but unambiguous assignment has not been made [113, 118]. The fourth transition is located near 6.08 eV (204 nm) and the fifth transition is located near 6.59 eV (188 nm); the intensity of both peaks is strong [11, 114–116]. The existence of the $n\pi^*$ transitions near 5.21, 6.32, and 7.08 eV (238, 196, and 175 nm) in guanine has been tentatively suggested by Clark [116]. In an elegant study on the transition moment directions of guanine, Clark [116] has suggested that the transition moment directions of 4.46, 5.08, 6.20 and 6.57 eV region peaks would be –12°, 80°, 70° and –10°, respectively with respect to the C4C5 direction (see Figure 14-1 for details). Using the R2PI spectroscopy, the spectral origins corresponding to the first singlet $\pi\pi^*$ transition of guanine tautomers are measured in the laser desorbed jet-cooled beam of the sample [41, 42, 44]. According to the reassigned R2PI spectra [44], the spectral origin of enol-N9H-trans, keto-N7H-IMINO-cis, keto-N7H-IMINO and enol-N7H forms tautomers [45] are at 4.31, 4.20, 4.12 and 4.07 eV, respectively.

In the case of aqueous solution of adenine the main absorption transition appears at 4.75 eV (261 nm) and this is short axis polarized. A weak shoulder near 4.64 eV

(267 nm) is also observed and this transition is long axis polarized [119]. In fact these two transitions are the component of the 4.77 eV (260 nm) main absorption band of adenine which are not resolved in the vapor phase and in a trimethyl phosphate solution [11, 37]. It should be noted that splitting between these two components is increased in the crystal environment of adenine compared to that in the water solution [119]. In the photoacoustic spectra, four absorption peaks are observed in the 180–300 nm region [120]. Transition moment directions of adenine have been studied extensively [11, 37] and an elegant analysis, to model electronic spectra of adenine, was performed by Clark [121, 122]. It was revealed that the 265 nm transition of adenine is polarized at 25° with respect to the C4C5 direction (see Figure 14-1) and the weak transition near 275 nm is polarized close to the long molecular axis. Holmen et al. [123] have also studied the transition moments of 9-methyladenine and 7-methyladenine oriented in the stretched polymer film. Clark [124] has tentatively assigned the existence of $n\pi^*$ transitions near 5.08 and 6.08 eV in the crystal of 2′-deoxyadenosine. The existence of an $n\pi^*$ transition near 5.38 eV was also revealed in the stretched polymer film of 9-methyladenine [123]. Recently several high level spectroscopic investigations were performed to study the spectral origins corresponding to the $\pi\pi^*$ and $n\pi^*$ transitions of adenine. Based on the REMPI and fluorescence investigations of supersonic jet-cooled adenine, Kim et al. [125] have suggested that the first transition of adenine has $n\pi^*$ character and the second has the $\pi\pi^*$ character; the spectral origins are located at 35503 cm^{-1} (~281.7 nm, ~4.40 eV), and 36108 cm^{-1} (~276.9 nm, ~4.48 eV), respectively. However, Luhrs et al. [126], based upon the similar study on adenine and 9-methyladenine, do not support the assignment of the $n\pi^*$ transition suggested by Kim et al. [125] and have speculated the involvement of some other tautomer in the latter study which might have formed due to heating of the sample. According to the investigation of Luhrs et al. [126] the spectral origins of the first $\pi\pi^*$ transition of adenine and 9MA are located at 36105 cm^{-1} (~277 nm, ~4.48 eV) and 36136 cm^{-1} (~276.7 nm, ~4.48 eV), respectively, and these results are in accordance with the observation made by Kim et al. [125]. Nir et al. [127] have found similar results based on the R2PI investigation of laser desorbed adenine.

The absorption spectra of aqueous solution of cytosine show broad peaks near 4.66 (266 nm) and 6.29 eV (197 nm) and weak peaks or shoulders near 5.39 (5.39 nm) and 5.85 eV (212 nm) [11, 113, 128–134]. In general, absorption spectrum of cytosine is solvent dependent [11, 129]. Compared to the first absorption peak of cytosine near 4.66 eV (266 nm) the corresponding peak of cytidine and 3-methycytosine are found to be near 4.57 (271 nm) and 4.29 eV (289 nm) respectively in aqueous solution [128, 132, 133]. Based upon the polarized reflection spectroscopy of single crystals of cytosine monohydrate, Clark and coworkers have assigned the transition moment directions of cytosine to be 6°, –46° and 76° for the first three transitions respectively and suggested two values (–27° or 86°) for the forth transition [131]. There is significant experimental and theoretical evidence for the existence of an $n\pi^*$ transition near 5.3 eV (232 nm) in cytosine [37]. Zaloudek et al. [131] have suggested the existence of another $n\pi^*$ transition near the 5.6 eV (220 nm).

The spectral features of uracil and thymine are generally similar having absorption bands near 4.77, 6.05 and 6.89 eV (260, 205 and 180 nm, respectively) [7, 11, 37]. The first and third absorption bands of thymine are generally slightly red-and blue-shifted with respect to the corresponding band in the uracil. The polarized absorption and reflection measurement show that the transition moment of the first band of uracil and thymine is about 0° and –20° respectively. Novros and Clark [135] have suggested 59° for the second transition and this conclusion was based on agreement with the results of the LD spectra of uracil [136]. Holmen et al. [137] have found 35° for the second transition in 1,3-dimethyluracil. The existence of an $n\pi^*$ transition within the first absorption envelope of uracil, thymine and their analogs has been suggested in several investigations [11, 120, 138, 139]. The relative position of the $n\pi^*$ transition is found to be solvent dependent. In the gas phase and in an aprotic solvent, the $n\pi^*$ state is the lowest but in the protic environment it has higher energy than that of the $\pi\pi^*$ state [11, 138, 139].

Theoretically, electronic singlet transition energy calculations of nucleic acid bases guanine, adenine, cytosine, thymine and uracil are performed at the CASPT2/CASSCF [140–142], TDDFT [143–150], RI-CC2 [151] and CIS [114, 143, 152–156] levels. In one of the TDDFT calculations, several set of diffuse functions were also used [145]. In comparing CIS transition energies, a scaling of 0.72 was found to be necessary and the scaled transition energies were found to be in good agreement with the corresponding experimental data [37, 114]. In general, computed transition energies were generally found to be in good agreement with the corresponding experimental data. Detailed discussion about the experimental and theoretical electronic transitions of nucleic acid bases can be found in the recent review article [37]. So and Alavi [157] have recently studied vertical transitions of DNA and RNA nucleosides at the TDDFT level using the B3LYP functional and the 6-311++G(d,p) and aug-cc-pVDZ basis sets. It was revealed that the sugar binding to isolated bases generally does not affect the nature of the lowest singlet $\pi\pi^*$ and $n\pi^*$ transitions of isolated bases significantly, but consequent to the sugar binding new low energy lying $n\pi^*$ and $\pi\sigma^*$ transitions are also obtained. Ritze et al. [158] have studied the effect of base stacking on the electronic transitions at the SAC-CI and RI-CC2 levels by considering cytosine-cytosine and thymine-thymine stacked dimers in the A- and B-DNA configuration. It should be noted that monomers are almost parallel in the B-conformation but significantly tilted in the A-conformation. It was revealed that the spectral splitting in thymine-thymine stacked dimer in the A-DNA is significantly (six times) larger than that in the B-DNA.

14.3.2. Electronic Transitions of Hypoxanthine

The absorption spectra of 9-methylhypoxanthine in the gas phase show peaks near 4.41, 5.19, 6.05 and 6.42 eV, in trimethylphosphate near 4.46, 5.02, 6.26 and 6.70 eV [129]. In water solution at pH of 6.1 the absorption spectra of 9-methylhypoxanthine show a broad shoulder in the range of 4.59–4.77 eV and peaks near 4.98 and 6.20 eV [129]. Further, the CD spectra of deoxyinosine 5′-phosphate

show a weak peak near 5.51 eV (225 nm) and this transition was suggested as being due to the existence of a weak $\pi\pi^*$ or $n\pi^*$ transition [113]. Detailed vertical electronic transition energy calculations were performed on hypoxanthine at the MCQDPT2/MCSCF, TD-B3LYP and CIS level and these energies are shown in the Table 14-1 along with the experimental data of 9-methylhypoxanthine [159]. It is evident that the MCQDPT2 transition energies are in good agreement with the experimental data within the accuracy of about 0.2 eV except for the second transition for which the margin of error is larger (Table 14-1). The computed transition energies of hypoxanthine at the TD-B3LYP level can also be correlated satisfactorily with the vapor phase experimental data, however, the margin of error is larger than for those obtained at the MCQDPT2 level. Computations also predict the existence of a weak $\pi\pi^*$ transition in the range of 6.2–6.3 eV at the TD-B3LYP level and at 5.48 eV at the MCQDPT2 level. Although, the existence of such a transition has neither been observed in the vapor spectra nor in aqueous solution, but the computed value is in the range of the CD transition of deoxyinosine 5′-phosphate near 5.51 eV [113]. The 5.48 eV transition obtained at the MCQDPT2 level in the gas phase is expected to be blue shifted in the hydrogen bonded environment, since the dipole moment of this state is lower than the ground state dipole moment at the CASSCF level. This transition is in excellent agreement with the CD prediction of the 5.51 eV region transition. Therefore, it appears that the computed results resolve the ambiguity concerning the nature of the 5.51 eV experimental transition in favor of the existence of a weak $\pi\pi^*$ transition.

14.3.3. Electronic Singlet Excited State Geometries

Ground state geometries of nucleic acid bases are generally planar except the amino group which is pyramidal. On the other hand, geometries in the lowest singlet $\pi\pi^*$ excited states are generally strongly nonplanar, except adenine which shows relatively less nonplanar excited state geometry [114]. In the S1($\pi\pi^*$) excited state the N9H tautomer of adenine is almost planar while the N7H tautomer of adenine has a nonplanar structure at the CIS/6-311G(d,p) level; the amino group is pyramidal for both tautomers [114]. A nonplanar structure around the N1C2N3 fragment of the N9H tautomer is revealed in the S1($n\pi^*$) excited state. Further, in this state the N7H tautomer has a structure reminiscent to twisted intramolecular charge transfer states [155, 160, 161]. The N7H tautomer has Cs symmetry; the amino hydrogens are at the dihedral angles of $\pm 61°$ with respect to the ring plane in this state. It should be noted that no significant intramolecular charge transfer was found [114]. In the case of the hydrated tautomers, where three water molecules were considered in the first solvation shell, water molecules were found to induce planarity in the system and consequently the ground and lowest singlet $\pi\pi^*$ excited state geometries were found to be almost planar including the amino group [114].

The S1($\pi\pi^*$) excited state geometry of the keto-N9H tautomer of guanine at the CIS/6-311G(d,p) level was found to be strongly nonplanar around the C6N1C2N3

Table 14-1. Computed and experimental transition energies (ΔE; eV), dipole moments (μ; Debye), oscillator strengths (f) and transition moment directions (Φ; °) according to Tinoco-DeVoe convention of hypoxanthine [159]

MCQDPT2	CASSCF		TD-B3LYP						Experimental[a]		
Isolated	Isolated		Isolated			Hydrated					
ΔE	ΔE	μ	ΔE	f	Φ	ΔE	f	Φ	ΔE^1	ΔE^2	ΔE^3
ππ* transitions											
4.63	5.62	2.66	4.75	0.139	−74	4.82	0.100	−78	4.41	4.46	4.59–4.77
5.35	6.55	4.66	5.43	0.146	43	5.36	0.141	41	5.19	5.02	4.98
5.48	6.92	3.80	6.22	0.003	−66	6.29	0.038	−3	5.51[b]		
5.78	7.97	5.87	6.44	0.065	34	6.34	0.023	24	6.05	6.26	6.20
6.31	8.40	6.83	6.89[c]	0.116	47	6.74	0.410	64	6.42	6.70	

[a] Absorption transition of 9-methylhypoxanthine, ΔE^1 =Vapor phase, ΔE^2 =in trimethylphosphate solution, ΔE^3 =in water at pH 6.1 [129]; [b] from the CD measurement of deoxyinosine 5′-phosphate [113]; [c] Rydberg contamination.

fragment [114]. The lowest singlet $n\pi^*$ excited state ($S1(n\pi^*)$) of the same tautomer and at the same level of the theory is characterized by the excitation of the C6=O lone pair electron. In this excited state the C6=O and N1H bonds are significantly out-of-plane from guanine ring and are opposite to each other. Further, the C6=O bond is increased by about 0.1 Å compared to the ground state value obtained at the HF/6-311G(d,p) level. The excited state geometrical distortion of the keto-N7H tautomer is similar to that of the keto-N9H form, but the amount of the distortion is usually smaller than that of the latter form. In the water solution modeled at the IEF-PCM approach and the CIS level of theory, although geometrical distortions were found similar to those on the gas phase, but the amount of change was significantly larger in the water solution [144]. The CASSCF [22] and TDDFT [23] levels have predicted significantly distorted $S1(\pi\pi^*)$ state geometry of the keto-N9H tautomer where the amino group and the C2 atom are significantly out-of-plane. But prediction regarding the keto-N7H tautomer in the excited state is significantly different. The CASSCF predicted significantly distorted geometry similar to that of the keto-N9H form [22] but TDDFT predicted a less distorted geometry [23]. On the other hand, CIS method predicted significantly nonplanar geometry for excited state of the keto-N7H tautomer, though the degree of nonplanarity is less than that of the keto-N9H tautomer in the same state [114].

At the CIS level of theory, the $S1(\pi\pi^*)$ the excited state geometry of cytosine (keto-N1H tautomer) revealed a significant nonplanarity mainly around the C4C5C6N1 fragment, the amino group is also significantly pyramidal in this state [114, 156]. In the lowest singlet $n\pi^*$ excited state ($S1(n\pi^*)$) the N3 atom is located significantly out-of-plane and considerable rotation of the amino group was also revealed. The obtained deformation was revealed as due to the result of excitation of lone pair electron of the N3 site and that of the partial mixing of the lone pair electron belonging to the amino nitrogen. Further, the N3 site provided the repulsive potential in the $S1(n\pi^*)$ excited state and therefore, the structure of hydration around the N3 site was completely modified in such state [114, 156].

The lowest singlet $n\pi^*$ excited state ($S1(n\pi^*)$) geometries of uracil and thymine were found to be slightly nonplanar at the CIS level of the theory, but the C4=O group is significantly out-of-plane and the C4=O bond is increased by about 0.1 Å compared to the ground state value [114, 162]. The $S1(\pi\pi^*)$ excited state geometry of thymine is in a boat type configuration where N1, C2, C4 and C5 atoms are in the approximate plane. For hydrated species, the structural deformations in the excited state are generally similar to those in isolated species [114, 162]. The CASSCF and RI-CC2 level of theoretical calculation with cc-pVDZ basis set also predicted significant elongation in the C4=O bond of thymine in the ($S1(n\pi^*)$) state and such elongation is large at the RI-CC2 level of the theory; with the ring geometry being only slightly distorted [24]. The $S1(\pi\pi^*)$ excited state geometry of thymine at the CASSCF/cc-pVDZ level is also reported but geometrical distortion was found to be significantly smaller than that obtained at the CIS level. However, a close examination of this geometry shows the significant elongation of the C2=O bond.

Thus, the reported geometry of the S1($\pi\pi^*$) excited state [24] appears significantly contaminated with nπ^* state characterized by the excitation of the lone pair electron of the C2=O group of thymine.

14.3.4. Excited State Proton Transfer in Purines

The electronic singlet excited state proton transfer reactions in guanine, adenine and hypoxanthine were also studied [163–165]. The keto-enol tautomerization reactions in guanine and hypoxanthine in the electronic lowest singlet $\pi\pi^*$ excited state were studied at the TDDFT/CIS level [163, 165]. Ground state geometries and transition states corresponding to the proton transfer from the keto to the enol form of guanine and hypoxanthine were optimized at the B3LYP/6-311++G(d,p) level. In the case of guanine, geometries in the excited state including that of the excited transition states were optimized at the CIS/6-311G(d,p) level [163]. The excited state geometries including that of the excited transition states in the case of hypoxanthine were optimized at the CIS/6-311++G(d,p) level [165]. The CIS optimized geometries were used to compute transition energies at the TD-B3LYP/6-311++G(d,p) level. Calculations were also performed for monohydrated species where a water molecule was placed in the proton transfer reaction path (between the N1-H and C6=O sites). The effect of bulk aqueous solvation was considered using the PCM solvation model. The transition state geometries in the excited state were found to be significantly nonplanar especially around the six-membered part the ring. Detailed discussion about excited state geometries can be found in [163, 165]. The computed ground and excited state proton transfer barrier height is shown in the Table 14-2. Evidently, the proton transfer barrier heights are significantly large in the ground and electronic singlet $\pi\pi^*$ excited states both in the gas phase and in bulk water solution. In the monohydrated species, where a water molecule was placed in the proton transfer reaction path, significant reduction in the barrier height was revealed. In general, the excited state barrier heights were revealed to be slightly larger than the corresponding ground state values. The transition states corresponding to the proton transfer from the keto to the enol form for the monohydrated forms were found to have zwitterionic structures. The transition state geometries of monohydrated complexes were in the forms of $H3O^+ \ldots X^-$ (X=guanine or hypoxanthine), except the N9H form of guanine in the excited state where water molecule is in the hydroxyl anionic form (OH^-) and the guanine is in the cationic form [163, 165]. On the basis of theoretical calculations it was suggested that the singlet electronic excitation of guanine and hypoxanthine may not facilitate the keto-enol tautomerization both in the gas phase and in the water solution. Salter and Chaban [164] have used MCQDPT2/MCSCF level of theory to investigate the proton transfer between the N9 and N3 sites of adenine both in the ground and electronic singlet excited states. The excited state proton transfer barrier height was found to be 43.0 kcal/mol while the corresponding ground state value was 63.0 kcal/mol. It is expected that the presence of a water molecule in the proton transfer reaction path may reduce the barrier significantly. This speculation was based on the fact that in the similar type of reaction

Table 14-2. Computed barrier height (kcal/mol) for guanine and hypoxanthine corresponding to the keto-enol tautomerism in the ground and the lowest singlet $\pi\pi^*$ excited state obtained at the B3LYP/6-311++G(d,p) and TD-B3LYP/6-311++G(d,p)//CIS/X levels, respectively in the gas phase and in aqueous solution [163, 165][a]

Species	Ground State		Excited State	
	Gas	Water	Gas	Water
	Guanine			
keto-N9H →TS-N9H	37.5	45.2	42.9	45.7
enol-N9H →TS-N9H	36.3	38.2	36.9	40.8
keto-N7H →TS-N7H	40.6	46.5	36.8	41.4
enol-N7H →TS-N7H	35.9	38.5	36.8	39.3
keto-N9H.H2O →TS-N9H.H2O	15.9	16.7	19.8	18.3
enol-N9H.H2O →TS-N9H.H2O	12.8	10.4	12.8	13.5
keto-N7H.H2O →TS-N7H.H2O	17.3	17.1	13.9	13.5
enol-N7H.H2O →TS-N7H.H2O	12.0	10.2	13.4	11.2
	Hypoxanthine			
keto-N9H →TS-N9H	39.85	47.15	50.98	55.67
enol-N9H →TS-N9H	35.87	38.83	30.28	30.29
keto-N7H →TS-N7H	42.99	48.53	47.93	51.27
enol-N7H →TS-N7H	35.76	39.27	28.49	30.29
keto-N9H.H2O →TS-N9H.H2O	17.05	17.46	26.09	23.17
enol-N9H.H2O →TS-N9H.H2O	12.62	10.17	8.41	4.54
keto-N7H.H2O →TS-N7H.H2O	18.22	17.83	33.79	28.31
enol-N7H.H2O →TS-N7H.H2O	11.84	9.91	15.05	7.93

[a] For guanine X=6-311G(d,p) and for hypoxanthine X=6-311++G(d,p).

in the 7-azaindole the barrier was found to be significantly reduced in the presence of a water molecule [166].

14.3.5. Hydration of Guanine

Hydration of guanine in the lowest singlet $\pi\pi^*$ excited state was studied recently [167]. In this investigation 1, 3, 5, 6 and 7 water molecules were considered in the first solvation shell of guanine. The ground state geometries of complexes were optimized at the HF/6-311G(d,p) level and that in the excited state were optimized at the CIS/6-311G(d,p) level. All geometries were found to be minima at the respective potential energy surfaces via harmonic vibrational frequency analysis. Geometry of guanine in the hydrated complexes in the ground state was found planar except the amino group which was pyramidal. But, water molecules involved in direct interaction with amino group were found to induce planarity and consequently the amino group of those complexes was revealed less pyramidal. In the excited state, the hydrogen bond distances were changed compared to the corresponding ground state values. Table 14-3 shows the selected dihedral angles of guanine showing structural nonplanarity in the excited state of isolated and hydrated complexes. It is evident from the data shown in the Table 14-3 that the degree of hydration has

Table 14-3. Selected dihedral angles (°) of the guanine in the isolated and hydrated forms and that in the GC and GG base pairs in lowest singlet $\pi\pi^*$ excited state obtained at the CIS/6-311G(d,p) level [167]

Parameters	G	G+1W	G+3W	G+5W	G+6W	GC	GG16	GG17
C6N1C2N3	64.0	−64.7	−64.8	38.1	43.0	36.4	3.1	−64.7
N1C2N3C4	−44.2	39.2	42.4	−1.7	−6.5	−3.3	−0.7	44.4
C2N3C4C5	2.4	2.0	0.0	−32.2	−29.0	−28.8	−1.3	−2.2
N3C4C5C6	18.5	−18.1	−18.8	32.2	29.7	29.6	1.1	−18.1
N1C6C5C4	0.6	−7.3	−3.3	2.6	5.4	2.6	1.0	−1.9
N2C2N3C4	161.4	−159.7	−160.5	−177.3	179.7	−177.7	−179.8	−156.9
H21N2C2N1	−42.3	31.0	34.8	10.2	10.6	3.7	8.2	41.6
H22N2C2N1	−171.8	167.9	170.4	−178.7	−177.4	−178.5	175.2	174.3

significant influence on the excited state structural nonplanarity of guanine. On the other hand, the excited state dynamics of guanine will depend upon the degree of hydration. It was found that the isolated, mono and trihydrated complexes have similar excited state geometrical deformation for guanine and these structural deformations are completely different than that obtained in the penta and hexahydrated guanine. Figure 14-2 shows the variation of NH stretching vibrational frequencies of isolated and hydrated guanine ground and excited state. It was revealed that the changes in stretching vibrations are in accordance with variation of hydrogen bond distances under electronic excitation compared to the corresponding ground state [167].

14.3.6. Electronic Excited States of Thiouracils

The thiosubstituted analogs of nucleic acid bases have been subjected to several investigations owing to their therapeutic and other biological activities [52, 168]. For example, thiouracil can be used as anticancer and antithyroid drugs. The investigation of t-RNA shows the presence of small amount of thiouracil [169, 170]. Comprehensive analysis of structures and properties of thiouracils can be found in the review article of Nowak et al. [168]. In general, all theoretical calculations suggest that in the gas phase and in water solution thiouracils (2-thiouracil (2TU), 4-thiouracil (4TU), 2,4-dithiouracil (DTU)) exist in the keto-thione/dithione tautomeric form. In the crystalline environment and in low temperature similar results were also obtained [171–174]. However, in ethanol solution 4TU has been suggested to occur in minor (thiol or enol) tautomeric form also [175] and this conclusion was based on the ab initio theoretical calculation and the electronic absorption and fluorescence spectra of the compound. On the basis of extensive absorption, circular dichroism (CD) and magnetic circular dichroism (MCD) spectroscopic investigations of 2TU, 4TU, DTU and their substituted analogs (Figure 14-3) in the water and acetonitrile solutions, Igarashi-Yamamoto [176] have indicated the presence of thiol tautomeric form for 2TU and DTU. Further, based on the NMR study of 2TU in deuterated dimethylsulfoxide solution the presence of thiol tautomeric form has been also suggested [177].

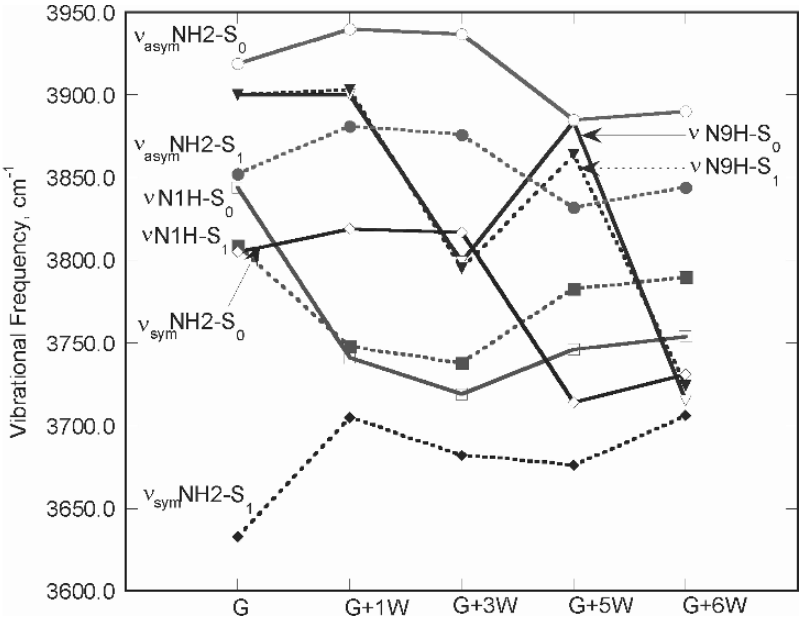

Figure 14-2. Variation of different stretching vibrational modes (unscaled values) of the guanine in the isolated and hydrated forms in the ground (HF/6-311G(d,p) level) and lowest singlet $\pi\pi^*$ excited state (CIS/6-311G(d,p) level). Reprinted with permission from ref. [167]. Copyright (2005) American Chemical Society

Significant change in the photophysical properties are revealed when the carbonyl group of a molecule is substituted by thiocarbonyl group. Consequently, the lowest singlet $\pi\pi^*$ and $n\pi^*$ states of thiocarbonyl containing molecules have significantly lower energy than the corresponding carbonyl containing molecules [178, 179].

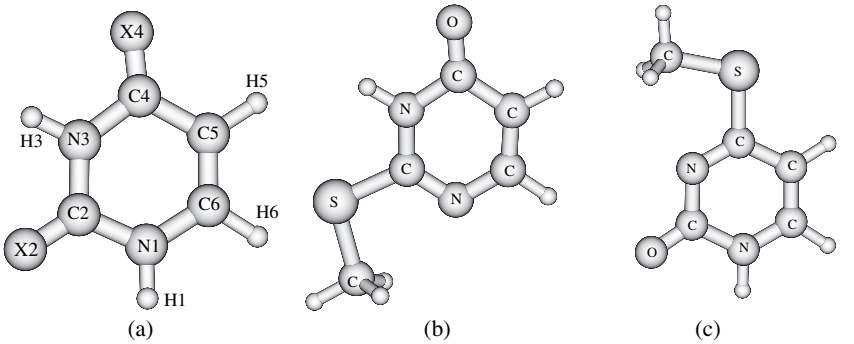

Figure 14-3. Atomic numbering scheme of 2TU (X2=S, X4=O), 4TU (X2=O, X4=S) and DTU (X2=X4=S). Different methyl derivatives can be obtained by the substitution of methyl group at the relevant site. Reprinted with permission from ref. [180]. Copyright (2004) American Chemical Society

Detailed theoretical electronic spectroscopic investigations were performed on thiouracils and their substituted analogs using the CIS, TDDFT (TDB3LYP) and MCQDPT2/MCSCF levels to explain the experimental transitions and to resolve the existing ambiguities regarding the presence of minor tautomers and the nature of singlet and triplet states [180–182]. The TDDFT transition energies were also computed in the water and acetonitrile solutions. In the case of 2TU, the computed transition energies at the TDB3LYP/6-311++G(d,p)//B3LYP/6-311++G(d,p) level were found to be in good agreement with the experimental transition energy data of 2TU and 2-thiouridine (2TUrd) [180]. The computed weak $\pi\pi^*$ transition in the 5.3–5.4 eV region were also found to be in good agreement with the experimental transition energy in the range of 5.1–5.3 eV which was only observed in the MCD spectra of 2TU and 2TUrd [176]. The computed transition energies of minor tautomers were also found to be in good agreement with the corresponding methyl substituted analog of 2TU. It was revealed that 2-methylthiouracil (2MTU) would exist in the N3H tautomeric form and this conclusion was based on the agreement with the transition energies of the thiol tautomer of 2TU (2TU-S2H1). Contrary to the conclusion drawn from the ref. [176], the first singlet $\pi\pi^*$ transition of 2TU and 2TUrd was not reveled to belong to the thiol form of 2TU.

The TDDFT computed transition energies of 4TU and different substituted methyl analogs were also found to be in good agreement with the corresponding experimental data [180]. The experimental CD band near 3.1 eV in 4TUrd in the acetonitrile solution which was assigned as due to the $n\pi^*$ transition was also supported from the TDDFT which yielded an $n\pi^*$ transition in the 3.2 eV region in the water and acetonitrile solution of 4TU and 1-methyl-4-thiouracil. The transition energy calculations of 4TU were also performed at the MCQDPT2/MCSCF level with 6-311+G(d) basis set and MP2/6-311++G(d,p) level optimized geometries [181]. The active space consisted of 12 orbitals where 6 were occupied π type while remaining were the π^* virtual type [181]. The changes in molecular electrostatic potentials consequent to electronic excitations were also studied. Good agreement between the MCQDPT2 transition energies and that of the experimental data were revealed. The effect of mono, di- and tri-hydrations were also studied in the lowest singlet $n\pi^*$ excited state of 4TU at the CIS/6-311++G(d,p) level. The lowest singlet $n\pi^*$ transition of 4TU was assigned to the excitation of lone-pair electron of the thiocarbonyl group. It was revealed that $n\pi^*$ excitation provides repulsive potential for hydrogen bonding [182]. On the basis of the agreement between the TDDFT computed transition energies and the corresponding experimental data, it was concluded that 2TU and 4TU will exist in the keto-thione tautomeric form.

Experimentally, the spectral profiles of DTU were found to be complex and solvent dependent [176]. The spectral profiles show two absorption peaks near 3.53 (351 nm) and 4.40 eV (282 nm) in the water solution, while three peaks near 3.53 (351 nm), 4.32 (287 nm) and 5.28 eV (235 nm) were obtained in the acetonitrile solution [176] The observed spectral transitions in the water and acetonitrile solutions of DTU were explained in terms of the thione-thiol tautomeric forms [176]. However, the relative stability of different tautomers of DTU at the

B3LYP/6-311++G(d,p) and MP2/cc-pVTZ/B3LYP/6-311++G(d,p) levels does not support the existence of thiol tautomers [180]. Further, the pK_a analysis of 2,4-dithiouridine has indicated the presence of an anionic and neutral form of DTU in the neutral solution [183]. Computed transition energies of DTU at the TDB3LYP/6-3111++G(d,p) level [180] were found to be in agreement with the corresponding experimental data. It was found that DTU will mainly exist in the dithione tautomeric form. Further, the existence of an anionic form of DTU obtained by the deprotonation of the N1H site of DTU was also revealed and probably this anionic form was responsible for the assignment of the thiol form of DTU in water and acetonitrile solution [176].

There are some contradictions regarding the nature of the first triplet state of thiouracils. The $n\pi^*$ state as the first triplet state of 4TUrd has been suggested by Salet et al. [184]. However, optically detected magnetic resonance (ODMR) investigation of 1-methyl-2-thiouracil, 1-methyl-4-thiouracil and 1-methyl-2,4-dithiouracil [185] and laser photolysis study of uracil, 4TUrd and 1,3-dimethyl-4-thiouracil in different solvents along with INDO/S calculations [186] have suggested the first triplet state of thiouracils as the $\pi\pi^*$ type. The MCQDPT2/MCSCF level of calculations on 4TU have also indicated that the $\pi\pi^*$ state is the lowest triplet state in the molecule [181]. Figure 14-4 shows that variation of lowest singlet and triplet transition energies of $n\pi^*$ and $\pi\pi^*$ type each for uracil and thiouracils computed at

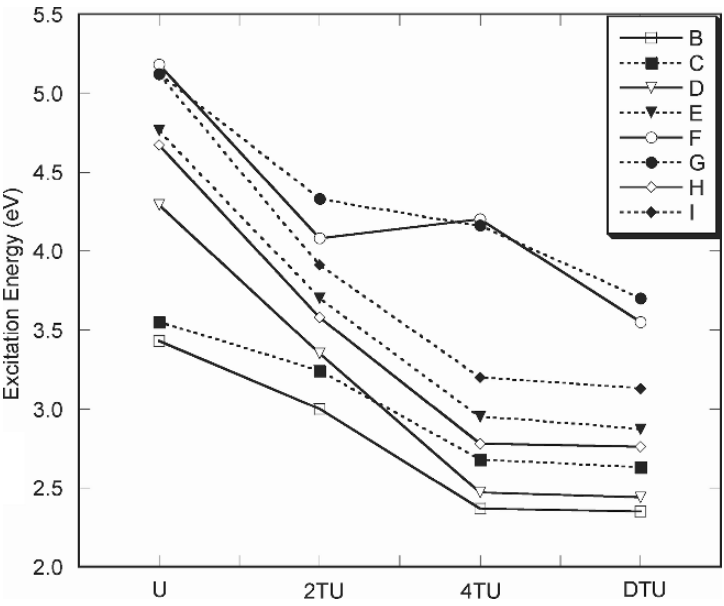

Figure 14-4. Variation of computed transition energies of uracil and thiouracils; B: $^3\pi\pi^*$ in gas, C: $^3\pi\pi^*$ in water, D: $^3n\pi^*$ in gas, E: $^3n\pi^*$ in water, F: $^1\pi\pi^*$ in gas, G: $^1\pi\pi^*$ in water, H: $^1n\pi^*$ in gas, and I: $^1n\pi^*$ in water. Reprinted with permission from ref. [180]. Copyright (2004) American Chemical Society

the TD-B3LYP/6-311++G(d,p)//B3LYP/6-311++G(d,p) level [180]. It is evident from the Figure 14-3 that for uracil and thiouracils the lowest $^3\pi\pi^*$ state has the lower energy than the $^3n\pi^*$ state both in the gas phase and in water solution and thus supporting the findings of Taherian and Maki [185] and Milder and Kliger [186] that the lowest triplet state of thiouracils is of the $\pi\pi^*$ type.

14.3.7. Excited States of Base Pairs

Ground and the lowest singlet $\pi\pi^*$ excited state geometries of the guanine-cytosine (GC) and guanine-guanine base pairs were also investigated at the HF and CIS levels using the 6-311G(d,p) basis set and computed results were compared with that of isolated guanine obtained at the same level of theory [187]. Two different hydrogen bonding configurations namely GG16 and GG17 of the guanine-guanine base pair were studied. In the GG16 base pair, guanine monomers form cyclic and symmetrical hydrogen bonds in between the N1H site of the first monomer and the carbonyl group of the second monomer, and vice versa. Whereas, the GG17 base pair is mainly connected by two strong hydrogen bonds; the amino group and the N1H site of the first guanine monomer acting as hydrogen bond donors (G_D) is hydrogen bonded with the carbonyl group and the N7 site of the second monomer acting as the hydrogen bond acceptor (G_A).

The electronic excitation to the lowest singlet $\pi\pi^*$ excited state of the GC base pair was found to be dominated by orbitals mainly localized at the guanine moiety while those for the GG17 base pair were found to be localized at the G_A monomer. In the case of the GG16 base pair, the orbitals involved in the lowest singlet $\pi\pi^*$ electronic excitation were found to be delocalized [187]. Geometries of base pairs are shown in the Figure 14-5 and selected geometrical parameters are shown in the Table 14-2. It was found that the amino groups of guanine belonging to the GC and GG16 base pairs are almost planar while that in the GG17 base pair is significantly pyramidal both in the ground state and in the lowest singlet $\pi\pi^*$ excited state. The excited state geometries of the isolated guanine and those of the GC and GG17 base pairs were found to be nonplanar and the predicted structural nonplanarity in the GC and GG17 base pairs was located at the excited guanine monomer. The remarkable difference was revealed in the mode of nonplanarity which was found to be significantly influenced by the hydrogen bonding in the

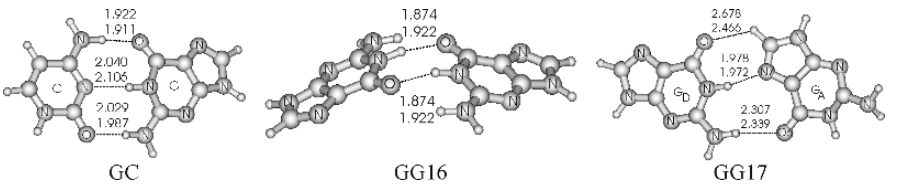

Figure 14-5. The S1($\pi\pi^*$) excited state geometries of GC, GG16 and GG17 base pairs. The top indices correspond to that in the ground state (HF/6-311G(d,p)) and bottom indices correspond to that in the S1($\pi\pi^*$) obtained at the CIS/6-311G(d,p) level

base pair. The geometrical deformation of isolated guanine and the G_A monomer of the GG17 base pair in the excited state were similar but found to be significantly different than the structural deformation of guanine monomer of the GC base pair in the excited state. The geometry of the GG16 base pair was predicted to be almost planar in the excited state except both guanine monomers are folded with respect to each other. Thus, this study also suggested that the excited state dynamics of bases and DNA may be significantly influenced by the hydrogen bonding environments. The interaction energy of the WC AT, AU and GC base pairs were also studied in the few lower lying singlet electronic excited states [97, 98]. In these investigations, the ground state geometries were optimized at the HF/6-31++G(d,p) level while the excited state geometries were optimized at the CIS/6-31++G(d,p) level by considering the planar molecular symmetry. The Boys-Bernardi counterpoise correction scheme [188] was utilized to compute excited state interaction energies. The computed interaction energies in the ground and singlet $\pi\pi^*$ excited state were found to be similar. However, the $n\pi^*$ excitations were found to significantly destabilize the hydrogen bonding in the studies systems. The reduction in the base pair energy in the WC GC base pair computed at the B3LYP level was also found in the triplet $\pi\pi^*$ state where excitation was localized at the guanine moiety [189]. But, the WC AT base pair was revealed to be unaffected under such excitation.

14.4. CONCLUSIONS

Molecules like nucleic acid bases and base pairs possess very complex photophysical and photochemical properties. Although, the excited state geometries of nucleic acid bases and base pairs can not be determine experimentally yet, theoretically the singlet excited state geometries are usually significantly nonplanar compared to the corresponding ground state. The electronic excitation energies of nucleic acid bases and base pairs under UV-irradiation are dissipated by ultrafast nonradiative channels probably operating through conical intersections between the excited and ground state potential energy surfaces assisted by structural nonplanarity and thus enabling these genetic molecules to be highly photostable. The degree of hydration usually affects the mode of excited state structural nonplanarity and therefore, it is expected that excited state dynamics will depend upon the degree of hydration. In DNA, hydrogen bonding and stacking interactions have important roles in deciding the fate of absorbed electronic energy. We hope that with the advancement in computational algorithms and computer hardware, it will be possible to study more complex nucleic acid fragments with reliable theoretical methods routinely.

ACKNOWLEDGEMENT

Authors are also thankful to financial supports from NSF-CREST grant No. HRD-0318519. Authors are also thankful to the Mississippi Center for Supercomputing Research (MCSR) for the generous computational facility.

REFERENCES

1. Avery OT, MacLeod CM, McCarthy M (1944) J Exp Med 79:137
2. Hershey A, Chase M (1952) Cold Spring Harb Symp Quant Biol 16: 445
3. Wilkins MHF, Stokes AR, Wilson HR (1953) Nature 171: 738.
4. Franklin RE, Gosling RG (1953) Nature 171: 740.
5. Watson JD, Crick FHC (1953) Nature 171: 737.
6. Schneider B, Berman HM (2006) In: Sponer J, Lankas F (eds) Computational Studies of RNA and DNA, in the series Challenges and Advances in Computational Chemistry and Physics, vol 2. Springer, The Neatherlands, p 1.
7. Crespo-Hernandez CE, Cohen B, Hare PM, Kohler B (2004) Chem Rev 104: 1977.
8. Schreier WJ, Schrader TE, Koller FO, Gilch P, Crespo-Hernandez CE, Swaminathan VN, Carell T, Zinth W, Kohler B (2007) Science 315: 625.
9. Boudaffa B, Cloutier P, Haunting D, Huels MA, Sanche L (2000) Science 287: 1658.
10. Bao X, Wang J, Gu J, Leszczynski J (2006) Proc Natl Acad Sci USA 103: 5658.
11. Callis PR (1983) Ann Rev Phys Chem 34: 329.
12. Duggan D, Bowmann R, Brodie BB, Udenfriend S (1957) Arch Biochem Biophys 68: 1.
13. Ge G, Zhu S, Bradrick TD, Georghiou S (1990) Photochem Photobiol 51: 557.
14. Georghiou S, Saim AM (1986) Photochem Photobiol 44: 733.
15. Agroskin LS, Korolev NV, Kulaev IS, Mesel MN, Pomashchinkova NA (1960) Dokl Akad Nauk SSSR 131: 1440.
16. Steele R.H, Szent-Gyorgyi A (1957) Proc Natl Acad Sci USA 43: 477.
17. Longworth JW (1962) Biochem J 84: 104P.
18. Bersohn R, Isenberg I (1964) J Chem Phys 40: 3175.
19. Eisinger J, Lamola AA (1971) In: Steiner RF, Weinryb I (eds) Excited State of Proteins and Nucleic Acids. Plenum Press, New York-London, p 107.
20. Saigusa H (2007) J Photochem Photobiol C 7: 197.
21. de Vries MS, Hobza P (2007) Annu Rev Phys Chem 58: 585.
22. Chen H, Li S (2006) J Phys Chem A 110: 12360.
23. Marian CM (2007) J Phys Chem A 111: 1545.
24. Perun S, Sobolewski AL, Domcke W (2006) J Phys Chem A 110: 13238.
25. Zgierski MZ, Patchkovskii S, Lim EC (2007) Can J Chem 85: 124.
26. Yarasi S, Brost P, Loppnow GR (2007) J Phys Chem A 111: 5130.
27. Blancafort L (2007) Photochem Photobiol 83: 603.
28. Kistler KA, Matsika S (2007) J Phys Chem A 111: 2650.
29. Chung WC, Lan Z, Ohtsuki Y, Shimakura N, Domcke W, Fujimura Y (2007) Phys Chem Chem Phys 9: 2075.
30. Barbatti M, Lischka H (2007) J Phys Chem A 111: 2852.
31. Yamazaki S, Kato S (2007) J Am Chem Soc 129: 2901.
32. Kundu LM, Loppnow (2007) Photochem Photobiol 83: 600.
33. Matsika S (2005) J Phys Chem A 109: 7538.
34. Markwick PRL, Doltsinis NL (2007) J Chem Phys 126: 175102
35. Markwick PRL, Doltsinis NL, Schlitter J (2007) J Chem Phys 126: 45104.
36. Groenhof G, Schafer LV, Boggio-Pasqua M, Goette M, Grubmuller H, Robb MA (2007) J Am Chem Soc 129: 6812.
37. Shukla MK, Leszczynski J (2007) J Biomol Struct Dyn 25: 93.
38. Leszczynski J (2000) In: Hargittai M, Hargittai I (eds) Advances in Molecular Structure and Research, vol 6. JAI Press Inc, Stamford, Connecticut, p 209.
39. Sponer J, Leszczynski J, Hobza P (2002) Biopolymers (Nucl Acid Sci) 61: 3.

40. Sponer J, Lankas F (2006) (eds) Computational Studies of RNA and DNA, in the series "Challenges and Advances in Computational Chemistry and Physics" vol 2. Springer, The Netherlands.
41. Nir E, Janzen Ch, Imhof P, Kleinermanns K, de Vries MS (2001) J Chem Phys 115: 4604.
42. Mons M, Dimicoli I, Piuzzi F, Tardivel B, Elhanine M (2002) J Phys Chem A 106: 5088.
43. Choi MY, Miller RE (2006) J Am Chem Soc 128: 7320.
44. Mons M, Piuzzi F, Dimicoli I, Gorb L, Leszczynki J (2006) J Phys Chem A 110: 10921.
45. Shukla MK, Leszczynski J (2006) Chem Phys Lett 429: 261.
46. Laxer A, Major DT, Gottlieb HE, Fischer B (2001) J Org Chem 66, 5463.
47. Chenon MT, Pugmire RJ, Grant DM, Panzica RP, Townsend LB (1975) J Am Chem Soc 97: 4636.
48. Lin J, Yu C, Peng S, Akiyama I, Li K, Lee LK, LeBreton PR (1980) J Am Chem Soc 102: 4627.
49. Nowak MJ, Rostkowska H, Lapinski L, Kwiatkowski JS, Leszczynski J (1994) J Phys Chem 98: 2813.
50. Hanus M, Kabelac M, Rejnek J, Ryjacek F, Hobza P (2004) J Phys Chem B 108: 2087.
51. Guerra CF, Bickelhaupt FM, Saha S, Wang F (2006) J Phys Chem A 110: 4012.
52. Stryer L (1988) Biochemistry 3rd edition Freeman, New York.
53. Holley RW, Apgar J, Everett GA, Madison JT, Marquisee M, Merrill SH, Penswick JR, Zamir A (1965) Science 147: 1462.
54. Grunberger D, Holy A, Sorm F (1967) Biochim Biophys Acta 134: 484.
55. Friedberg EC, Walker GC, Siede W (1995) DNA Repair and Mutagenesis, ASM Press, Washington, DC.
56. Ramaekers R, Maes G, Adamowicz L, Dkhissi A (2001) J Mol Struct 560: 205.
57. Sheina GG, Stepanian SG, Radchenko ED, Blagoi YuP (1987) J Mol Struct 158: 275.
58. Shukla MK, Leszczynski J (2000) J Phys Chem A 104: 3021.
59. Shukla MK, Leszczynski J (2000) J Mol Struct (Theochem) 529: 99.
60. Hernandez B, Luque FT, Orozco M (1996) J Org Chem 61: 5964.
61. Costas ME, Acevedo-Chavez R (1997) J Phys Chem A 101: 8309.
62. Lin J, Yu C, Peng S, Akiyama I, Li K, Lee LK, LeBreton PR (1980) J Phys Chem 84: 1006.
63. Lichtenberg D, Bergmann F, Neiman Z (1972) Isr J Chem 10: 805.
64. Munns ARI, Tollin P (1970) Acta Crystallogr B 26: 1101.
65. Sadeghi RR, Cheng H-P (1999) J Chem Phys 111: 2086.
66. Szczesniak M, Szczepaniak K, Kwiatowski JS, KuBulat K, Person WB (1998) J Am Chem Soc 110: 8319.
67. Kwiatkowski JS, Leszczynski J (1996) J. Phys. Chem. 100: 941.
68. Brown RD, Godfrey PD, McNaughton D, Pierlot AP (1989) J Am Chem Soc 111: 2308.
69. Drefus M, Bensaude O, Dodin G, Dubois JE (1976) J Am Chem Soc 98: 6338.
70. Nir E, Muller M, Grace LI, de Vries MS (2002) Chem Phys Lett 355: 59.
71. Smets J, Adamowicz L, Maes G (1996) J Phys Chem 100: 6434.
72. Lapinski L, Nowak MJ, Fulara J, Les A, Adamowicz L (1990) J Phys Chem 94: 6555.
73. McClure RJ, Craven BM (1973) Acta Crystallogr 29B: 1234.
74. Kobayashi R (1998) J Phys Chem A 102: 10813.
75. Trygubenko SA, Bogdan TV, Rueda M, Orozco M, Luque JF, Sponer J, Slavicek P, Hobza P (2002) Phys Chem Chem Phys 4: 4192.
76. Fogarasi G, Szalay PG (2002) Chem Phys Lett 356: 383.
77. Suwaiyan A, Morsy MA, Odah KA (1995) Chem Phys Lett 237: 349.
78. Morsy MA, Al-Somali AM, Suwaiyan A (1999) J Phys Chem B 103: 11205.
79. Rejnek J, Hanus M, Kabelac M, Ryjacek F, Hobza P (2005) Phys Chem Chem Phys 7: 2006.
80. Shishkin OV, Gorb L, Leszczynski J (2000) Chem Phys Lett 330: 603.

81. Shishkin OV, Gorb L, Hobza P, Leszczynski J (2000) Int J Quantum Chem 80: 1116.
82. Leszczynski J (1992) Int J Quantum Chem 19: 43.
83. Dong F, Miller RE (2002) Science 298: 1227.
84. Li X, Cai Z, Sevilla MD (2002) J Phys Chem A 106: 1596.
85. Lin J, Yu C, Peng S, Akiyama I, Li K, Lee LK, LeBreton PR (1980) J Am Chem Soc 102: 4627.
86. Yang X, Wang X-B, Vorpagel ER, Wang L-S (2004) Proc Natl Acad Sci USA 101: 17588.
87. Trofimov AB, Schirmer J, Kobychev VB, Potts AW, Holland DMP, Karlsson L (2006) J Phys B At Mol Opt Phys 39: 305.
88. Close DM (2004) J Phys Chem A 108: 10376.
89. Crespo-Hernandez CE, Arce R, Ishikawa Y, Gorb L, Leszczynski J, Close DM (2004) J Phys Chem A 108: 6373.
90. Cauet E, Dehareng D, Lievin J (2006) J Phys Chem A 110: 9200.
91. Podolyan Y, Gorb L, Leszczynski J (2000) J Phys Chem A 104: 7346.
92. Huang Y, Kenttamaa H (2004) J Phys Chem A 108: 4485.
93. Kryachko ES, Nguyen MT, Zeegers-Huyskenes T (2001) J Phys Chem A 105: 1288.
94. Ganguly S, Kundu KK (1994) Can J Chem 72: 1120.
95. Benoit R, Frechette M (1986) Can J Chem 64: 2348.
96. Greco F, Liguori A, Sindona G, Uccella N (1990) J Am Chem Soc 112: 9092.
97. Shukla MK, Leszczynski J (2002) J Phys Chem A 106: 1011.
98. Shukla MK, Leszczynski J (2002) J Phys Chem A 106: 4709.
99. Gorb L, Podolyan Y, Dziekonski P, Sokalaski WA, Leszczynski J (2004) J Am Chem Soc 126: 10119.
100. Podolyan Y, Nowak MJ, Lapinski L, Leszczynski J (2005) J Mol Struct 744: 19.
101. Kurita N, Danilov VI, Anisimov VM (2005) Chem Phys Lett 404: 164.
102. Sponer J, Florian J, Hobza P, Leszczynski J (1996) J Biomol Struct Dyn 13: 827.
103. Dabkowska I, Jurecka P, Hobza P (2005) J Chem Phys 122: 204322.
104. Sponer J, Jurecka P, Hobza P (2004) J Am Chem Soc 126: 10142.
105. Jurecka P, Sponer J, Cerny J, Hobza P (2006) Phys Chem Chem Phys 8: 1985.
106. Sponer J, Jurecka P, Marchan I, Luque FJ, Orozco M, Hobza P (2006) Chem Eur J 12: 2854.
107. Zendlova L, Hobza P, Kabelac M (2006) Chem Phys Chem 7: 439.
108. Kumar A, Mishra PC, Suhai S (2005) J Phys Chem A 109: 3971.
109. Kumar A, Knapp-Mohammady M, Mishra PC, Suhai S (2004) J Comput Chem 25: 1047.
110. Lind MC, Bera PP, Richardson NA, Wheeler SE, Schaefer HF, III (2006) Proc Natl Acad Sci USA 103: 7554.
111. Sutherland JC, Griffin K (1984) Biopolymers 23: 2715.
112. Voelter W, Records R, Bunnenberg E, Djerassi C (1968) J Am Chem Soc 90: 6163.
113. Sprecher CA, Johnson Jr WC (1977) Biopolymers 16: 2243.
114. Shukla MK, Leszczynski J (2003) In: Leszczynski J (ed) Computational Chemistry: Reviews of Current Trends, vol 8. World Scientific, Singapore, p 249.
115. Clark LB (1977) J Am Chem Soc 99: 3934.
116. Clark LB (1994) J Am Chem Soc 116: 5265.
117. Santhosh C, Mishra PC (1989) J Mol Struct 198: 327.
118. Miles DW, Hann SJ, Robins RK, Eyring H (1968) J Phys Chem 72: 1483.
119. Stewart RF, Davidson J (1963) J Chem Phys 39: 255.
120. Inagaki T, Ito A, Heida K, Ho T (1986) Photochem Photobiol 44: 303.
121. Clark LB (1989) J Phys Chem 93: 5345.
122. Clark LB (1990) J Phys Chem 94: 2873.
123. Holmen A, Broo A, Albinsson B, Norden B (1997) J Am Chem Soc 119: 12240.

124. Clark LB (1995) J Phys Chem 99: 4466.
125. Kim NJ, Jeong G, Kim YS, Sung J, Kim SK, Park YD (2000) J Chem Phys 113: 10051.
126. Luhrs DC, Viallon J, Fischer I (2001) Phys Chem Chem Phys 3: 1827.
127. Nir E, Kleinermanns K, Grace L, de Vries MS (2001) J Phys Chem A 105: 5106.
128. Voet D, Gratzer WB, Cox RA, Doty P (1963) Biopolymers 1: 193.
129. Clark LB, Tinoco I (1965) J Am Chem Soc 87: 11.
130. Yamada T, Fukutome H (1968) Biopolymers 6: 43.
131. Zaloudek F, Novros JS, Clark LB (1985) J Am Chem Soc 107: 7344.
132. Johnson Jr WC, Vipond PM, Girod JC (1971) Biopolymers 10: 923.
133. Kaito A, Hatano M, Ueda T, Shibuya S (1980) Bull Chem Soc Jpn 53: 3073.
134. Raksany K, Foldvary I (1978) Biopolymers 17: 887.
135. Novros JS, Clark LB (1986) J Phys Chem 90: 5666.
136. Matsuoks Y, Norden B (1982) J Phys Chem 86: 1378.
137. Holmen A, Broo A, Albinsson B (1994) J Phys Chem 98: 4998.
138. Becker RS, Kogan G (1980) Photochem Photobiol 31: 5.
139. Fujii M, Tamura T, Mikami N, Ito M (1986) Chem Phys Lett 126: 583.
140. Fulscher MP, Serrano-Andres L, Roos BO (1997) J Am Chem Soc 119: 6168.
141. Lorentzon J, Fulscher MP, Roos BO (1995) J Am Chem Soc 117: 9265.
142. Fulscher MP, Roos BO (1995) J Am Chem Soc 117: 2089.
143. Mennucci B, Toniolo A, Tomasi J (2001) J Phys Chem A 105: 4749.
144. Mennucci B, Toniolo A, Tomasi J (2001) J Phys Chem A 105: 7126.
145. Shukla MK, Leszczynski J (2004) J Comput Chem 25: 768.
146. Tsolakidis A, Kaxiras E (2005) J Phys Chem A 109: 2373.
147. Varsano D, Felice RD, Marques MAL, Rubio A (2006) J Phys Chem B 110: 7129.
148. Cerny J, Spirko V, Mons M, Hobza P, Nachtigallova D (2006) Phys Chem Chem Phys 8: 3059.
149. Improta R, Barone V (2004) J Am Chem Soc 126: 14320.
150. Gustavsson T, Banyasz A, Lazzarotto E, Markovitsi D, Scalmani G, Frisch MJ, Barone V, Improta R (2006) J Am Chem Soc 128: 607.
151. Fleig T, Knecht S, Hattig C (2007) J Phys Chem A 111: 5482.
152. Shukla MK, Mishra PC (1999) Chem Phys 240: 319.
153. Shukla MK, Mishra SK, Kumar A, Mishra PC (2000) J Comput Chem 21: 826.
154. Mishra SK, Shukla MK, Mishra PC (2000) Spectrochim Acta 56A: 1355.
155. Broo A (1998) J Phys Chem A 102: 526.
156. Shukla MK, Leszczynski J (2002) J Phys Chem A 106: 11338.
157. So R, Alavi S (2007) J Comput Chem 28: 1776.
158. Ritze H-H, Hobza P, Nachtigallova D (2007) Phys Chem Chem Phys 9: 1672.
159. Shukla MK, Leszczynski J (2003) J Phys Chem A 107: 5538.
160. Andreasson J, Holmen A, Albinsson B (1999) J Phys Chem B 103: 9782.
161. Mennucci B, Toniolo A, Tomasi J (2000) J Am Chem Soc 122: 10621.
162. Shukla MK, Leszczynski J (2002) J Phys Chem A 106: 8642.
163. Shukla MK, Leszczynski J (2005) J Phys Chem A 109: 7775.
164. Salter LM, Chaban GM (2002) J Phys Chem A 106: 4251.
165. Shukla MK, Leszczynski J (2005) Int J Quantum Chem 105: 387.
166. Chaban GM, Gordon MS (1999) J Phys Chem A 103: 185.
167. Shukla MK, Leszczynski J (2005) J Phys Chem B 109: 17333.
168. Nowak MJ, Lapinski L, Kwiatkowski JS, Leszczynski J (1997) In: Leszczynski J (ed) Computational Chemistry: Reviews of Current Tends, vol 2, World Scientific, Singapore, p 140.
169. Lipsett MN (1965) J Biol Chem 240: 3975.

170. Yaniv M, Favre A, Barrell BG (1969) Nature 223: 1331.
171. Tiekink ERT (1989) Z Kristallogr 187: 79.
172. Hawkinson SW (1975) Acta Crystallogr B31: 2153.
173. Shefter E, Mautner HG (1967) J Am Chem Soc 89: 1249.
174. Rostkowska H, Szczepaniak K, Nowak MJ, Leszczynski J, KuBulat K, Person KB (1990) J Am Chem Soc 112: 2147.
175. Rubin YV, Morozov Y, Venkateswarlu D, Leszczynski J (1998) J Phys Chem A 102: 2194.
176. Igarashi-Yamamoto N, Tajiri A, Hatano M, Shibuya S, Ueda T (1981) Biochim Biophys Acta 656: 1.
177. Kokko JP, Goldstein JH, Mandell L (1962) J Am Chem Soc 84: 1042.
178. Pownall HJ, Schaffer AM, Becker RS, Mantulin WM (1978) Photochem Photobiol 27: 625.
179. Capitanio DA, Pownall HJ, Huber JR (1974) J Photochem 3: 225.
180. Shukla, MK and Leszczynski J (2004) J Phys Chem A 108: 10367.
181. Shukla, MK and Leszczynski J (2004) J Phys Chem A 108: 7241.
182. Shukla, MK and Leszczynski J (2006) J Mol Struct (Theochem) 771: 149.
183. Faerber P, Saenger W, Scheit KH, Suck D (1970) FEBS Lett 10: 41.
184. Salet C, Bensasson R, Favre A (1983) Photochem Photobiol 38: 521.
185. Taherian M-R, Maki AH (1981) Chem Phys 55: 85.
186. Milder SJ, Kliger DS (1985) J Am Chem Soc 107: 7365.
187. Shukla MK, Leszczynski J (2005) Chem Phys Lett 414: 92.
188. Boys SF, Bernardi F (1970) Mol Phys 19: 553.
189. Noguera M, Blancafort L, Sodupe M, Bertran J (2006) Mol Phys 104: 925.